Supplementary information to:

Tissue factor and PAR1 promote microbiota-induced intestinal vascular remodelling

Christoph Reinhardt, Mattias Bergentall, Thomas U. Greiner, Florence Schaffner, Gunnel Östergren-Lundén, Lars C. Petersen, Wolfram Ruf, and Fredrik Bäckhed

Content:

Supplementary Fig. 1

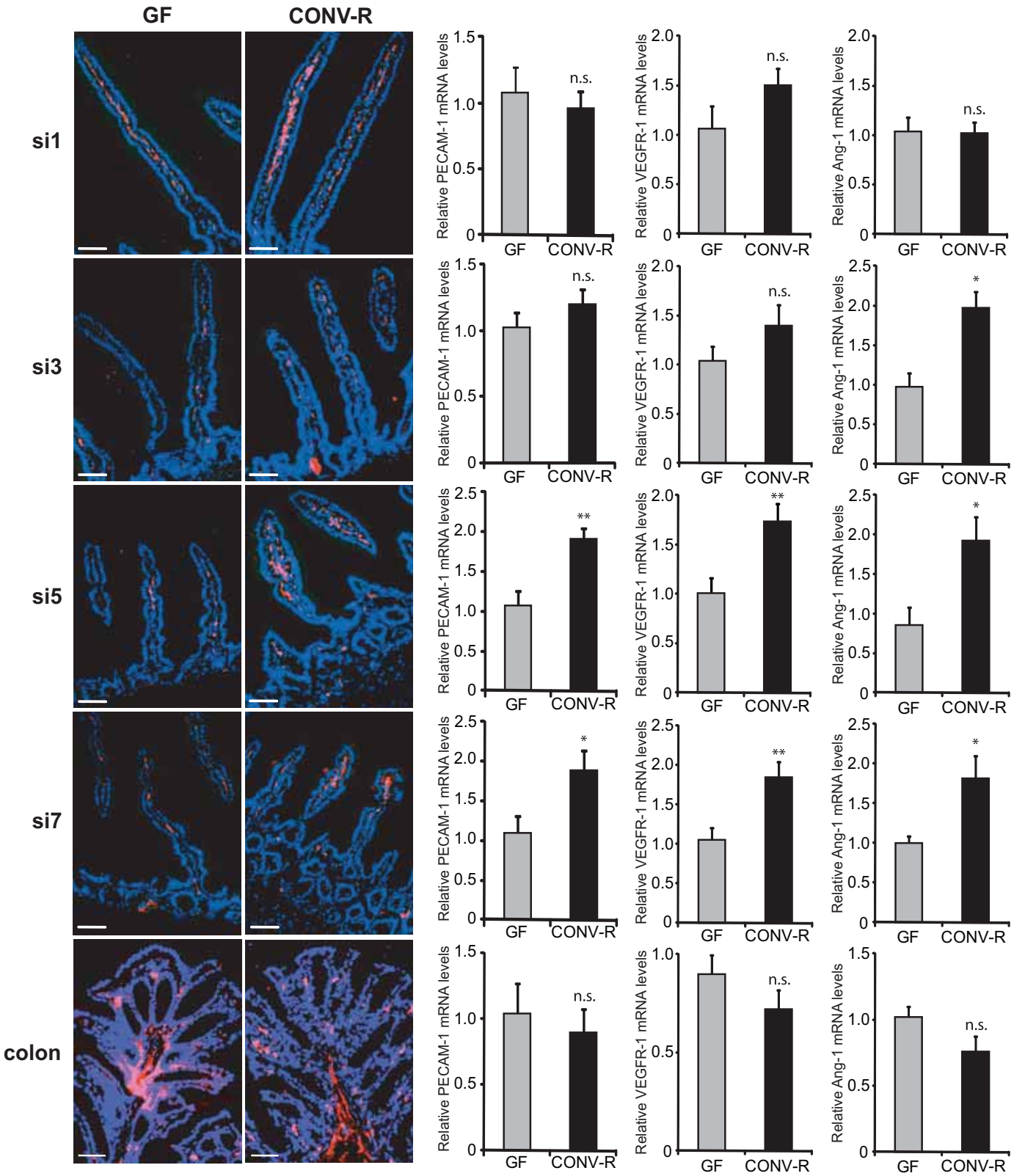

Supplementary Fig. 1. Vascularization along the length of the gut. PECAM-1 staining (red) of intestinal segments (small intestine divided in 8 equal-sized segments and first third of the colon) from GF and CONV-R mice. Nuclei were stained with Hoechst nuclear dye (blue). Scale bars = 50 μm. Relative mRNA levels of the vascular markers PECAM-1 and VEGFR-1 and the angiogenic factor Ang-1 in GF and CONV-R mice (n = 4–8 mice/group). Mean values ± s.e.m. are plotted. *P < 0.05; ** P< 0.01.

Supplementary Fig. 2

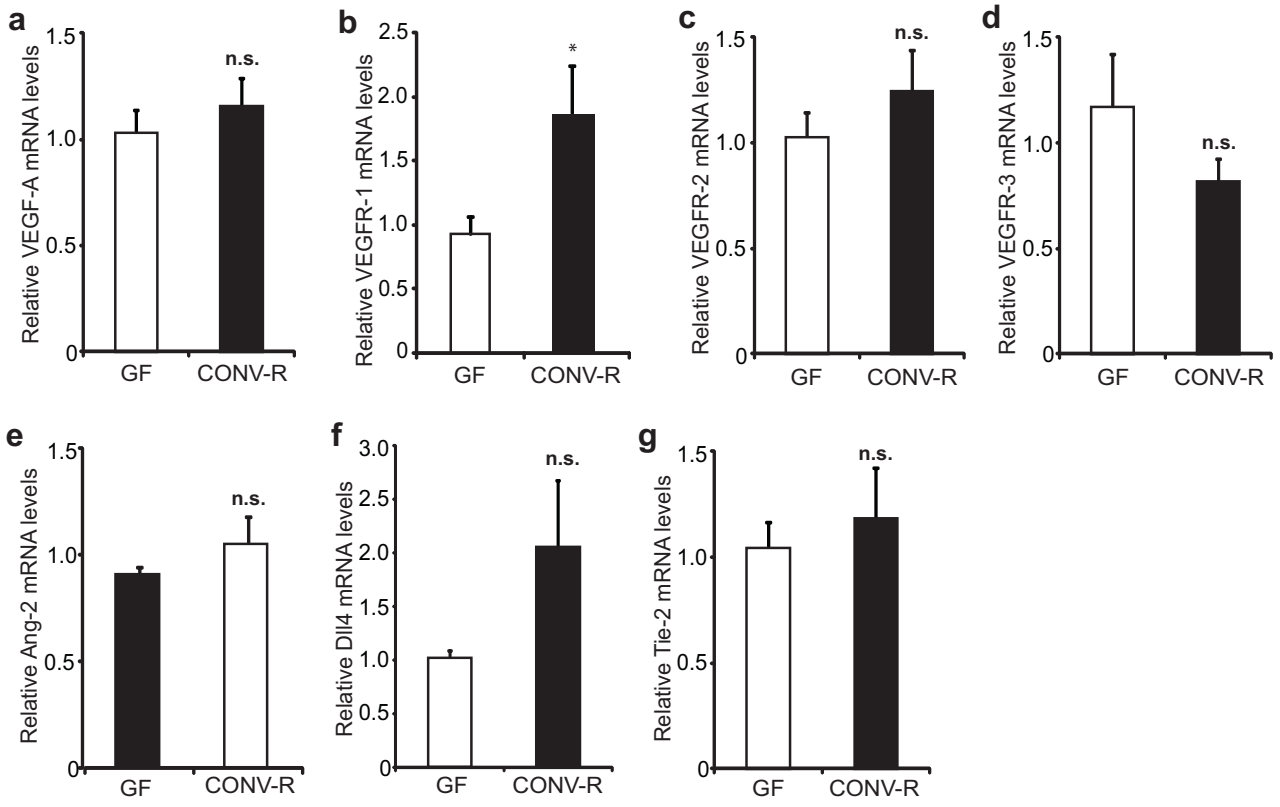

Supplementary Fig. 2. a-g, Quantification of small intestinal mRNA expression levels of VEGF-A, VEGFR-1, VEGFR-2, VEGFR-3, Ang-2, Dll4 and Tie-2 in GF and CONV-R mice (n = 5-11).

Supplementary Fig. 3

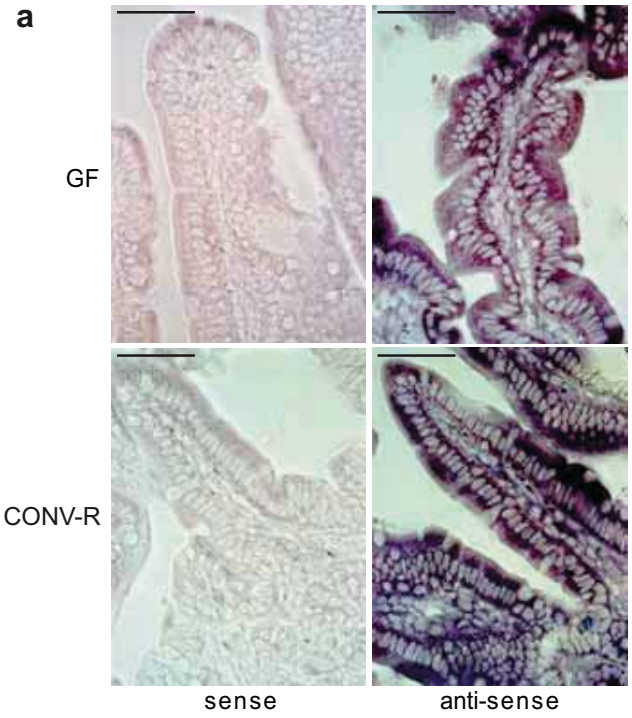

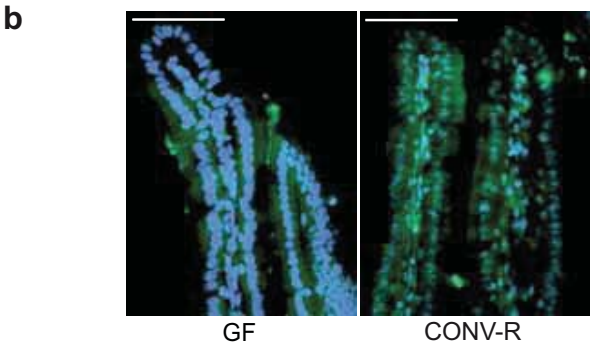

Supplementary Fig. 3. TF is expressed by enterocytes. a, In situ hybridization and **b,** Immunohistochemistry of mouse TF in small intestinal tissue from Swiss Webster mice reveals enterocytes as major sites of small intestinal TF expression. Scale bars = 50 μm.

Supplementary Fig. 4

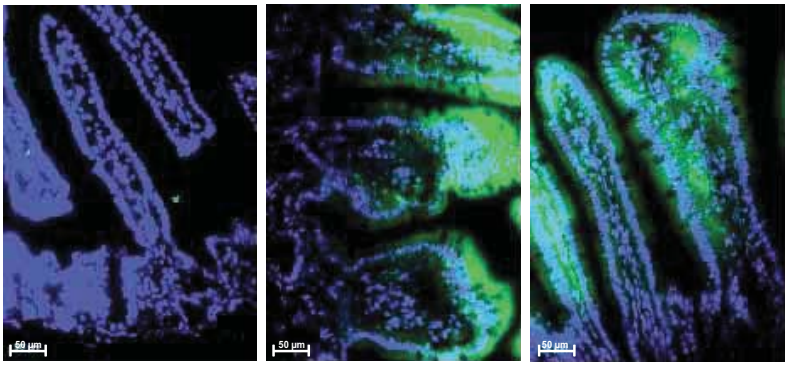

CONV-D | CONV-D + control Ab | CONV-D + anti-TF

Supplementary Fig. 4. Intraperitoneally injected antibodies target the small intestine. Alexa 488-anti-rabbit immunostaining of small intestinal tissue in Swiss Webster mice treated with control or anti-TF antibodies. Scale bars = 50 µm.

Supplementary Fig. 5

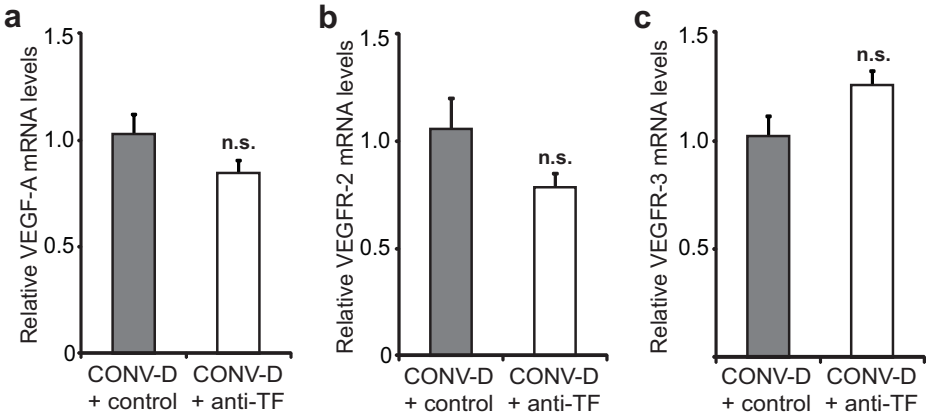

Supplementary Fig. 5. Anti-TF treatment does not affect mRNA levels of VEGF-A, VEGFR-2 or VEGFR-3 in the small intestine. qRT-PCR analysis of **a**, VEGF-A, **b,** VEGFR-2, and **c,** VEGFR-3 in the small intestine from CONV-D Swiss Webster mice reveals no differential expression induced by treatment with anti-TF (n = 5-6 mice/group). Mean values ± s.e.m. are plotted.

Supplementary Fig. 6

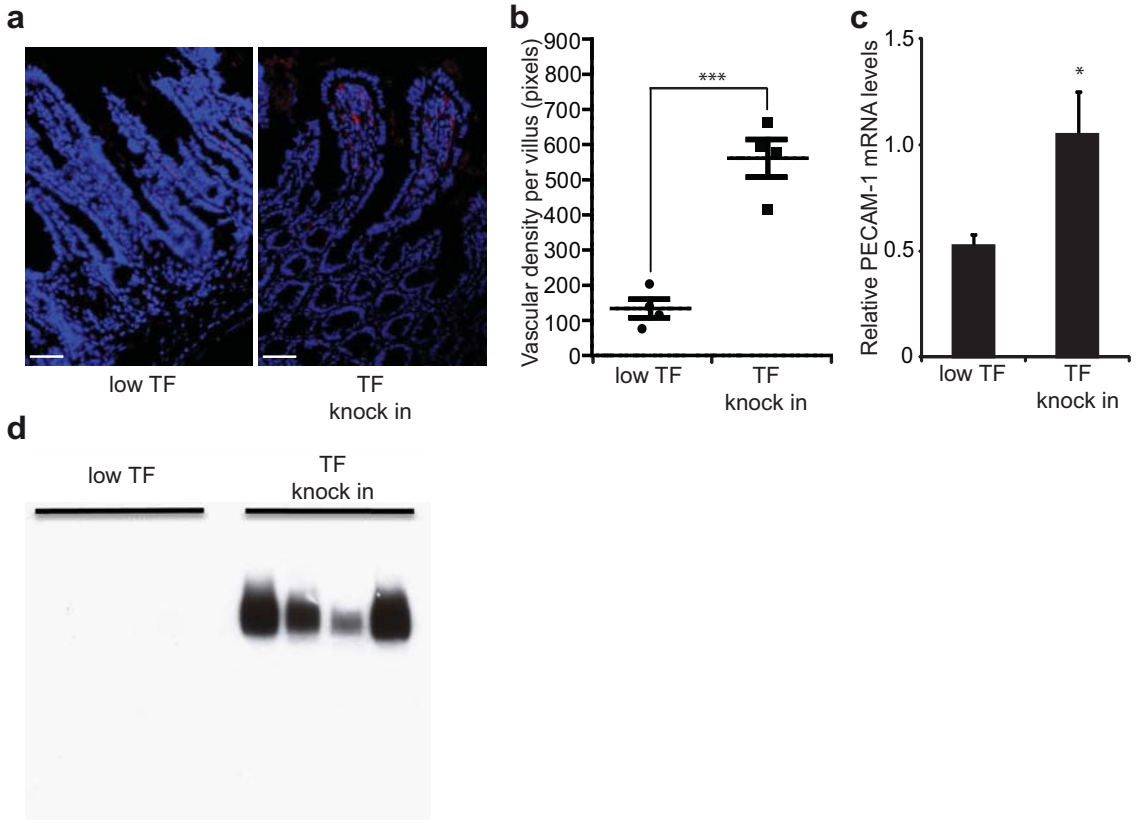

Supplementary Fig. 6. Low TF mice have reduced levels of PECAM-1 in the small intestine. **a,** PECAM-1 staining of small intestinal sections from hypomorphic low-TF and TF knock in mice. **b,** Quantification of **a** (n = 4 mice/group). **c**, Relative PECAM-1 mRNA levels in small intestinal sections from low TF and TF knock in mice (n = 4-5 mice/group). **d,** Verification of the TF knock in. TF in the small intestine was immuno-precipitated with human TF-specific antibody 5G9. Immunoprecipitated TF was detected by western blotting with goat anti-human TF (n = 4 mice/group).

Supplementary Fig. 7

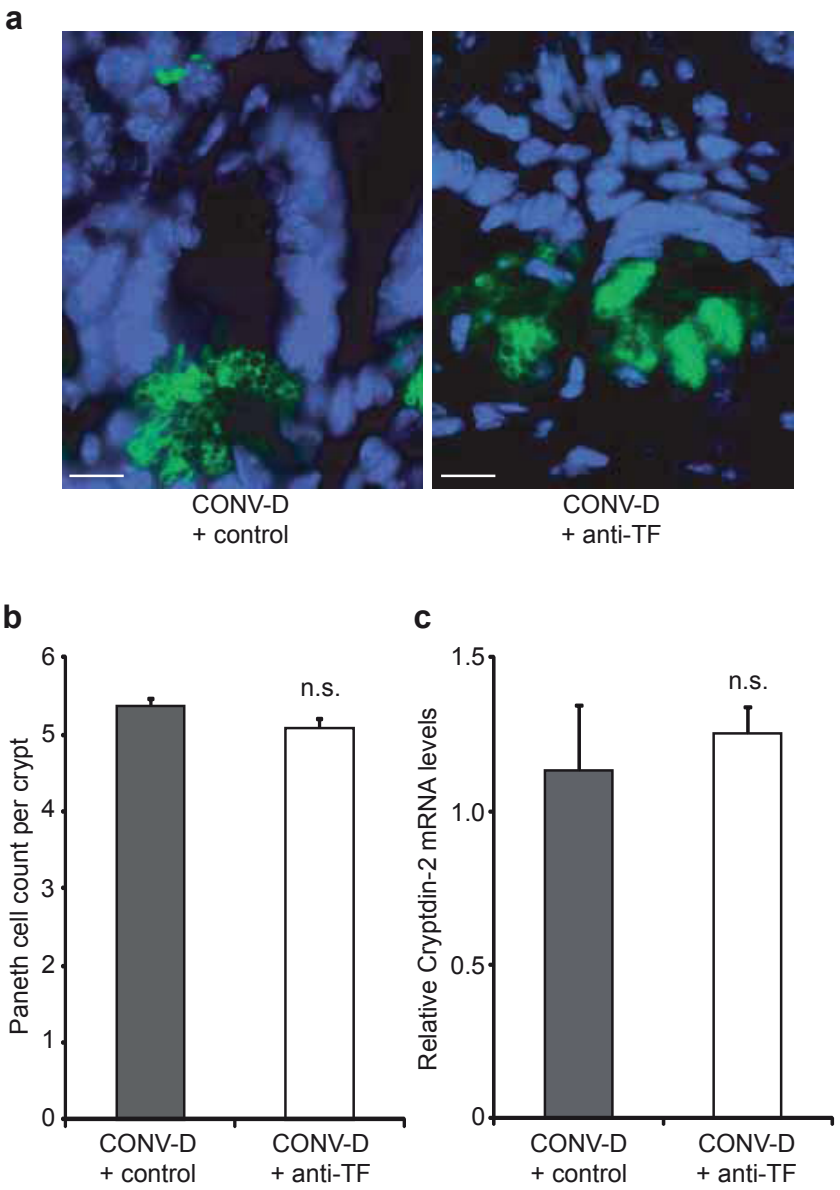

Supplementary Fig. 7. Anti-TF treatment does not affect Paneth cell number. **a,** FITC-Isolectin stain of small intestinal Paneth cells localized at the bottom of each crypt. Scale bar = 10 μm. **b,** Number of Paneth cells per small intestinal crypt in mice treated with isotype control antibody or with anti-TF antibody (n = 5 mice / group). **c,** Relative mRNA levels of the Paneth cell marker Cryptdin-2 in the small intestine (n=6 mice/group). Female Swiss Webster mice were used in all panels. Mean values ± s.e.m. are plotted.

Supplementary Fig. 8

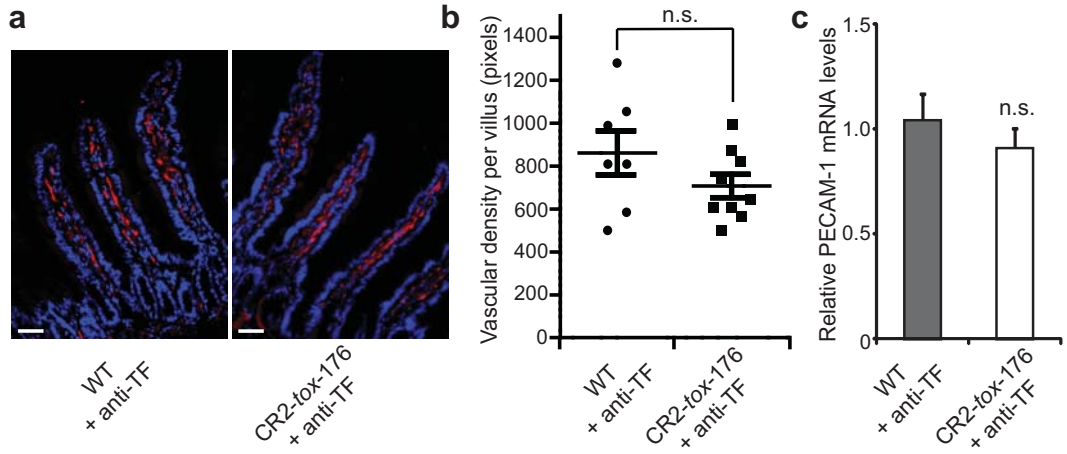

Supplementary Fig. 8. Similar vascular density in mice that lack Paneth cells and their wild-type littermates following treatment with anti-TF. a. PECAM-1 staining (red) of small intestinal sections from anti-TF-treated WT mice and anti-TF-treated CR2-*tox*-176 mice on a FUB/N genetic background that lack Paneth cells. Nuclei were stained with Hoechst nuclear dye (blue).
b. Quantification of **a** (n = 7-9 mice/group). c. Relative mRNA levels of the vascular marker PECAM-1 in anti-TF-treated WT mice and anti-TF-treated CR2-*tox*-176 mice (n = 7-9 mice/group). Scale bars = 50 μm. Mean values ± s.e.m. are plotted.

Supplementary Fig. 9

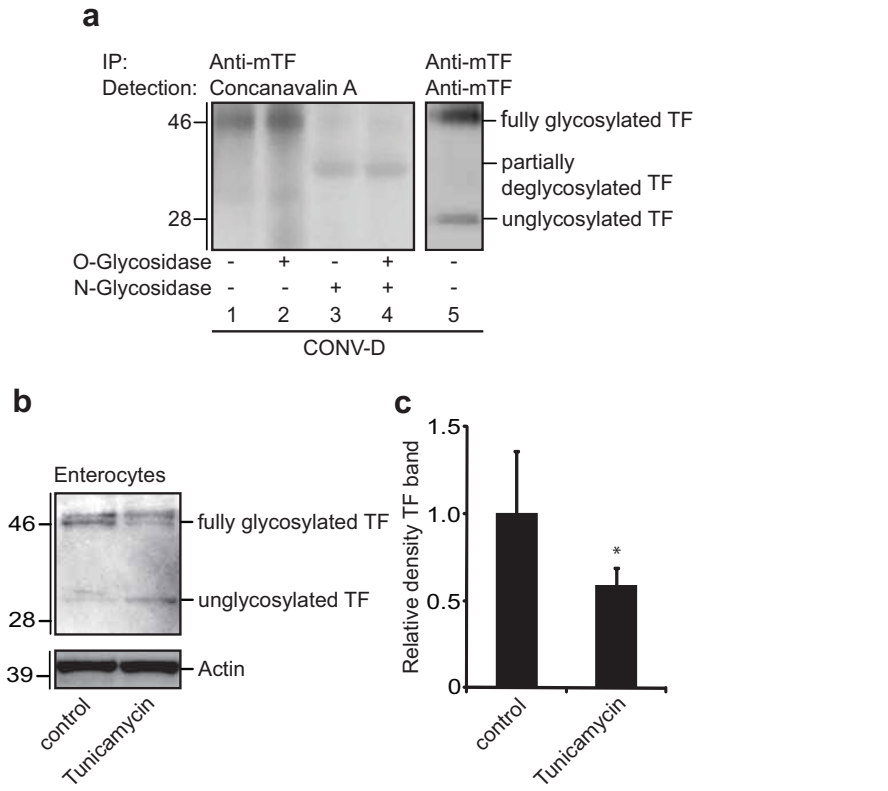

Supplementary Fig. 9. TF is N-glycosylated. a, Detection of mannose residues using concanavalin A on TF after immunoprecipitation with anti-TF antibody and treatment with glycosidases in small intestinal lysates from CONV-D mice. Note that concanavalin A did not recognize the unglycosylated form of TF. **b**, Anti-TF immunoblot of primary enterocytes (from CONV-R mice) incubated in the absence and presence of tunicamycin (10 µmol/l) for 2 h. **c**, Quantification of b (n = 5 mice/group).

Supplementary Fig. 10

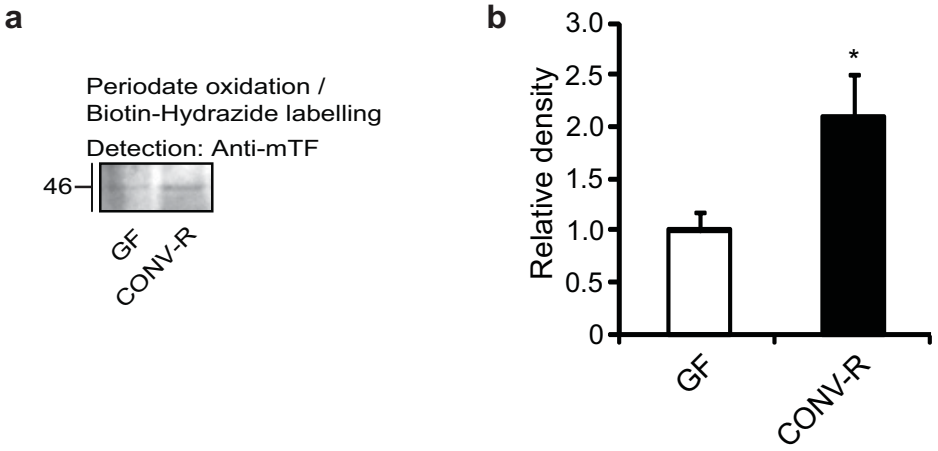

Supplementary Fig. 10. Increased surface localization of glycosylated TF in colonized mice. a, Enterocytes from GF and CONV-R Swiss Webster mice were isolated and surface carbohydrates were labeled with biotin-hydrazide after periodate oxidation followed by pull-down with streptavidin and immunoblotting with anti-TF antibody. **b,** Quantification of **a** (n = 5 mice/group). * $P < 0.05$

Supplementary Fig. 11

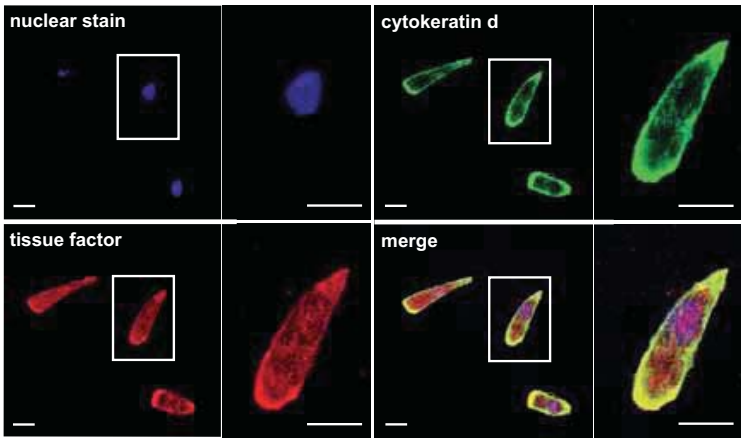

Supplementary Fig. 11. TF is expressed on the cell surface of enterocytes. Confocal immunofluorescence imaging of primary enterocytes isolated from CONV-R mice. Scale bars = 10 μm.

Supplementary Fig. 12

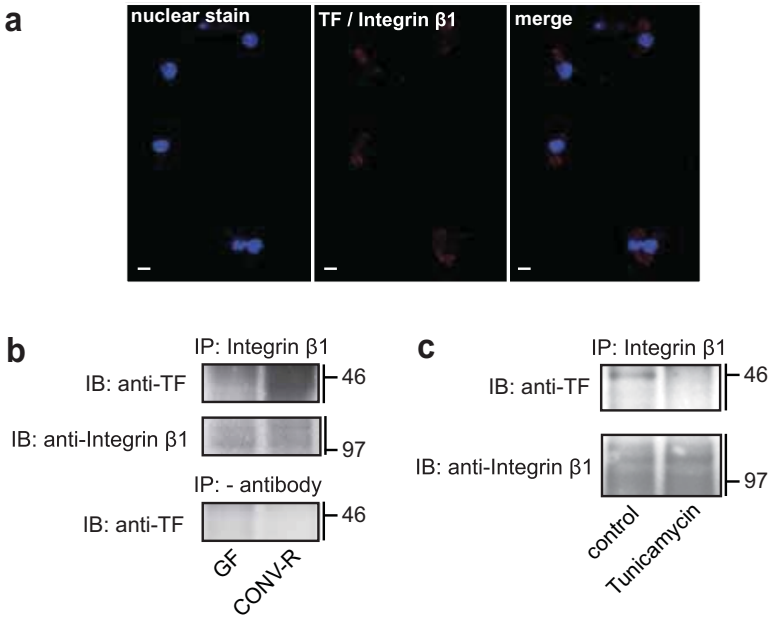

Supplementary Fig. 12. Increased TF-integrin association in colonized mice.
a, Proximity ligation assay reveals co-localization of TF with β1 integrin in isolated primary enterocytes from CONV-R mice. Co-immunoprecipitation of TF with β1 integrin in small intestinal lysates from **b**, GF and CONV-R mice and **c**, CONV-R mice intraperitoneally injected with DMSO (control) and or tunicamycin (1 mg/kg body weight). Cells or small intestinal samples from Swiss Webster mice were used in all panels. Scale bars = 10 μm.

Supplementary Fig. 13

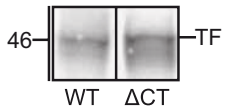

Supplementary Fig. 13. Deletion of the cytoplasmic domain does not affect expression of TF. TF immunoblot of small intestinal tissue from WT and ΔCT mice on a C57Bl6/J genetic background. Note that deletion of the cytoplasmic domain removes only ~ 2 kDa of the 25 kDa core protein.This reduction in mass has little effect on the mobility of the protein, which is highly glycosylated in the extracellular domain.

Supplementary Fig. 14

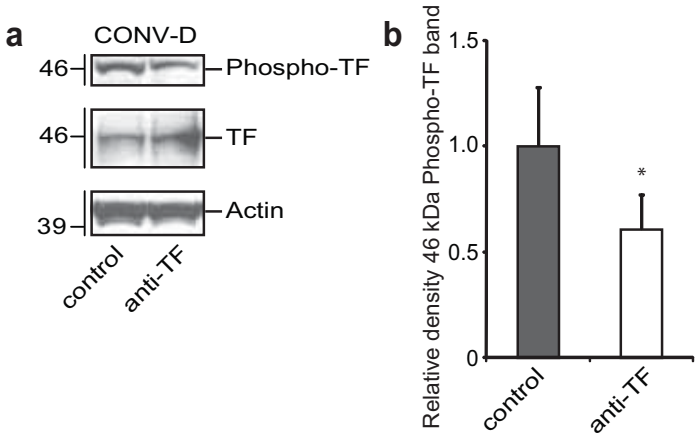

Supplementary Fig. 14. Anti TF-treatment reduces TF-phosphorylation. a, Anti-TF and anti-phospho-TF immunoblots of small intestinal lysates from CONV-D mice treated with control or anti-TF antibody. **b**, Quantification of a (n = 7 mice/group).
Mean values ± s.e.m. are plotted. *P < 0.05.

Supplementary Fig. 15

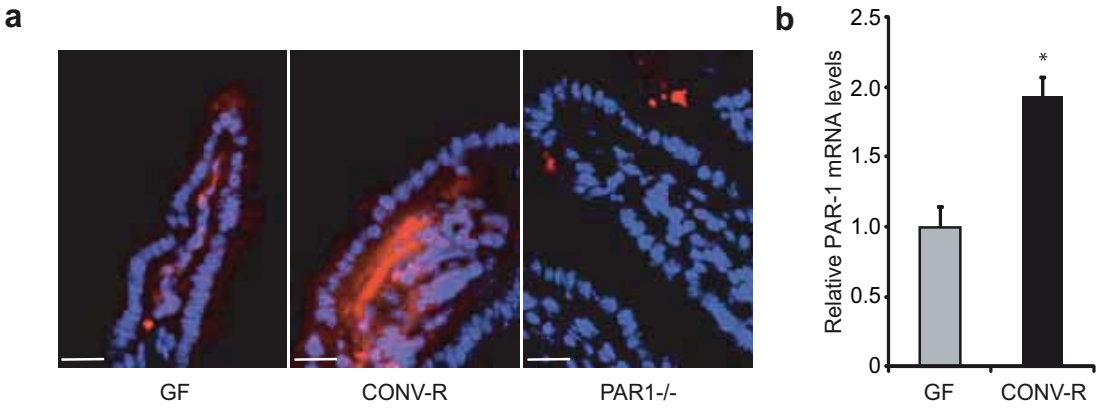

Supplementary Fig. 15. PAR1 is expressed in enterocytes and endothelial cells in the small intestine. a, PAR1 staining (red) of small intestinal tissue from GF and CONV-R Swiss Webster mice. Tissue from PAR1-/- mice were used as a specificity control. Scale bars = 20 μm. **b,** qRT-PCR analysis of PAR1 expression in isolated primary enterocytes from GF and CONV-R Swiss Webster mice (n = 10-11 mice). Mean values ±s.e.m. are plotted. * P <0.05.

Supplementary Fig. 16

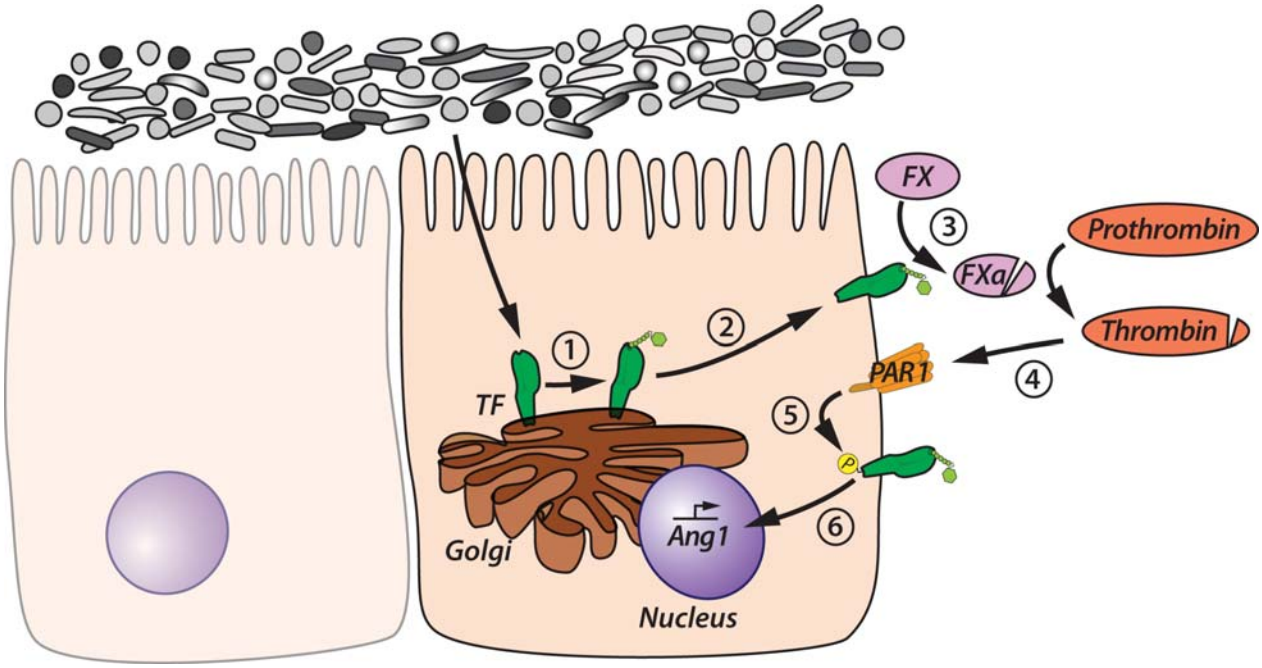

Supplementary Fig. 16. Proposed mechanism for microbiota-induced vascular remodelling. (1) The gut microbiota promotes glycosylation and (2) cell surface localization of TF. (3) Surface localized TF generates FXa, (4) which is required for thrombin generation. (5) PAR-1 activation results in TF phosphorylation, (6) which is associated with increased Ang1 expression.

Supplementary Fig. 17

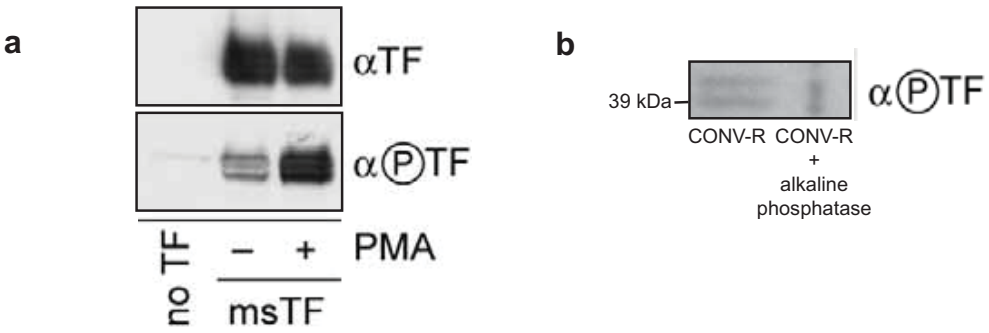

Supplementary Fig. 17. Antibody reagents to detect phosphorylation of mouse TF. a, Antibodies were raised in rabbits to purified mouse TF extracellular domain expressed in *Escherichia coli* and to KLH coupled synthetic peptide corresponding to Ser/Thr phosphorylated mouse cytoplasmic domain. Western blotting of HUVEC lysates transduced without or with mouse TF expressing adenovirus. Cells were stimulated for 1 h with PMA to induce TF phosphorylation. **b,** Phosphatase control. Small intestinal lysates from CONV-R Swiss Webster mice were incubated with 100 units of alkaline phosphatase. TF-phosphorylation was detected with the antibody raised against Ser/Thr phosphorylated mouse cytoplasmic domain.

Supplementary table 1. Primer sequences used in this study.

Gene	Forward primer	Reverse primer	Amplicon length
TF	AAC CCA CCA ACT ATA CCT ACA CT	GTC TGT GAG GTC GCA CTC G	101 bp
PECAM-1	CTG CCA GTC CGA AAA TGG AAC	CTT CAT CCA CTG GGG CTA TC	218 bp
VEGFR-1	GAG GAG GAT GAG GGT GTC TAT AGG T	GTG ATC AGC TCC AGG TTT GAC TT	116 bp
VEGFR-2	GCC CTG CTG TGG TCT CAC TAC	CAA AGC ATT GCC CAT TCG AT	114 bp
VEGFR-3	CTG GCA AAT GGT TAC TCC ATG A	ACA ACC CGT GTG TCT TCA CTG	182 bp
VEGF-A	AGT CCC ATG AAG TGA TCA AGT TCA	ATC CGC ATG ATC TGC ATG G	220 bp
Ang-1	CAT TCT TCG CTG CCA TTC TG	GCA CAT TGC CCA TGT TGA ATC	103 bp
Ang-2	CAG CCA CGG TCA ACA ACT C	CTT CTT TAC GGA TAG CAA CCG AG	123 bp
Defcr-2 (Cryptdin-2)	CTG CTC ACC AAT CCT CCC A	GCC TGG ACC TGA AAG GAC AGT A	267 bp
PAR-1	TGA ACC CCC GCT CAT TCT TTC	CCA GCA GGA CGC TTT CAT TTT T	105 bp
PAR-2	CAT GTT CAA TTA CTT CCT CTC ACT	GGT TTT AAC ACT GGT TGA GCT TGA	472 bp
asTF	TTC CTC ACC CTG CGG CAA GTC T	AGT GTT TCT TTC CCG TGC TTG AGC C	85 bp
Dll4	GGA ACC TTC TCA CTC AAC ATC C	CTC GTC TGT TCG CCA AAT CT	141 bp
Tie-2	GAG TCA GCT TGC TCC TTT ATG G	AGA CAC AAG AGG TAG GGA ATT G	77 bp
L32	CCT CTG GTG AAG CCC AAG ATC	TCT GGG TTT CCG CCA GTT T	102 bp